Energy &
Environmental
Science

Using reverse osmosis membranes to control ion transport during water electrolysis

Journal:	*Energy & Environmental Science*
Manuscript ID	EE-ART-07-2020-002173.R1
Article Type:	Paper
Date Submitted by the Author:	19-Aug-2020
Complete List of Authors:	Shi, Le; Penn State, Civil & Environmental Engineering Rossi, Ruggero; Penn State SON, MOON; Penn State, Civil & Environmental Engineering Hall, Derek; Penn State, EMS Energy Institute Hickner, Michael; Penn State, Department of Materials Science and Engineering Gorski, Christopher; Penn State, Civil and Environmental Engineering Logan, Bruce; Penn State, Civil & Environmental Engineering

Date: August 17, 2020
Submitted to: *Energy Env. Sci.*

Using reverse osmosis membranes to control ion transport during water electrolysis

Le Shi[1], Ruggero Rossi[1], Moon Son[1], Derek M. Hall[2], Michael A. Hickner[3], Christopher A. Gorski[1], & Bruce E. Logan[1]
[1]Department of Civil and Environmental Engineering, The Pennsylvania State University, University Park, PA, USA.
[2]Department of Energy and Mineral Engineering, The Pennsylvania State University, University Park, PA, USA.
[3]Department of Materials Science and Engineering, The Pennsylvania State University, University Park, PA, USA.

The decreasing cost of electricity produced using solar and wind and the need to avoid CO_2 emissions from fossil fuels has heightened interest in hydrogen gas production by water electrolysis. Offshore and coastal hydrogen gas production using seawater and renewable electricity is of particular interest, but it is currently economically infeasible due to the high costs of ion exchange membranes and the need to desalinate seawater in existing electrolyzer designs. A new approach is described here that uses relatively inexpensive commercially available membranes developed for reverse osmosis (RO) to selectively transport favorable ions. In an applied electric field, RO membranes have a substantial capacity for proton and hydroxide transport through the active layer while excluding salt anions and cations. A perchlorate salt was used to provide an inert and contained anolyte, with charge balanced by proton and hydroxide ion flow across the RO membrane. Synthetic seawater (NaCl) was used as the catholyte, where it provided continuous hydrogen gas evolution. The RO membrane resistance was 21.7 ± 3.5 Ω cm^2 in 1 M NaCl and the voltages needed to split water in a model electrolysis cell at current densities of 10-40 mA cm^{-2} were comparable to those found when using two commonly used, more expensive ion exchange membranes.

Introduction

Hydrogen gas accounts for 1% of global energy use,[1, 2] with 50 billion kg of gas produced globally each year (~53% for fertilizer). Hydrogen gas production could increase in the future due to its potential uses in transportation and energy storage. Reducing fossil fuel consumption and CO_2 emissions associated with H_2 production can be accomplished using renewable energy sources, such as solar and wind. Although the cost of H_2 produced by water electrolysis is currently dominated by electricity prices, electrolyzer capital costs will become increasingly important in the future.[3] To make H_2 production by water electrolysis economically competitive to H_2 produced from methane, the costs of the membrane (commonly a cation exchange membrane, CEM) and the catalyst layer used in most direct water electrolysis systems must be decreased, as they contribute to nearly half of the cost of the electrolysis cell stack.[4] A second barrier to affordable H_2 gas production by water electrolysis is the location of the renewable energy. Offshore and coastal sites are especially of interest for H_2 production to link locations with affordable wind or solar arrays with abundant seawater.[5-7] However, the direct use of seawater as an electrolyte in contact with the anode results in the production of high concentrations of chlorine gas and other toxic chlorinated compounds (e.g. chlorine, chlorine radicals, and other forms of oxidized chlorine) that can damage membranes.[6, 8, 9] Therefore, it is currently necessary to first desalinate water before electrolysis to avoid chloride oxidation and to use either highly acidic CEMs which restrict catalyst use to noble metals or use highly alkaline solutions with anion exchange membranes (AEMs).[6, 7, 10, 11] Current efforts to directly use seawater have been primarily directed at developing electrodes with large overpotentials for chloride oxidation to facilitate oxygen evolution,[12-14] but this approach has not yet achieved commercial success. Asymmetric electrolyte feeds, using an alkaline KOH anolyte and seawater catholyte has also recently been proposed, but this approach required the use of relatively expensive AEMs that can degrade in alkaline solutions.[15-17]

Here, we demonstrate a different approach for improving the economic viability of water electrolysis using synthetic seawater based on repurposing low-cost reverse osmosis (RO) membranes to replace expensive CEMs. The cost of the RO membranes (<\$10 m^{-2}) is an order of magnitude less than CEMs (~ \$500 – \$1000 m^{-2}), providing a path for greatly decreasing membrane costs for water electrolyzer systems. In addition, RO membranes can be highly selective for small ions, allowing transport of protons (diameter of 0.20 nm, in the form of H_3O^+) and OH^- ions (0.22 nm) through the membrane to sustain current generation with an applied potential while excluding the passage of larger ions such as Na^+ and Cl^- .[18, 19] The RO membrane can restrict the passage of large salt ions from the anolyte, allowing the use of an asymmetric anolyte that does not result in the generation of chlorine gas and other strong oxidizers (HOCl and OCl^-), which could damage the membrane.[20] For example, perchlorate salts or acids are often used as electrolytes in electrochemical studies because chlorine is fully oxidized and therefore stable, enabling selective water oxidation by the oxygen evolution reaction to produce only O_2. Saline water, such as seawater, can be used as the catholyte without needing to be desalinated as it is kept separated from the anode by the RO membrane. When using these two different electrolytes the anolyte rapidly becomes slightly acidic, increasing the concentration of protons for transport across the membrane, while the catholyte pH increases with hydrogen gas evolution occurring under relatively alkaline conditions. Typical RO membranes can be operated over a pH range of 2-11,[21] and thus strongly acidic or alkaline solutions need to be avoided. This approach of using moderately acidic or basic solutions in the presence of other competing anions and cations is fundamentally different from current water electrolysis methods in which both electrolytes are either highly acidic or alkaline and all other ions are excludes from the solutions.

While diffusive ion transport in RO membranes has been extensively studied during pressure-driven water desalination,[22] relatively little is known on ion transport with an applied electric field in the absence of an appreciable water flux[23] as only a few studies have been conducted in the absence of an appreciable water flux.[24-26] Because of the unique structure of the thin film composite membrane that retains larger ions, but allows a pressure driven water flux, a thin film membrane has the potential to break the trade-off between ionic conductivity and selectivity that occurs for ion exchange membranes.[27, 28] Evidence for the potentially unique applications of RO thin film membranes is provided by results with thin film nanofiltration (NF) membranes that have shown differences in specific ion permeabilities (e.g. Na^+ versus Mg^{2+}) in the presence and absence of pressure driven flow,[23] and improved performance in flow batteries compared to ion exchange membranes due to better vanadium ion retention coupled with high proton conductivity (3 M H_2SO_4 electrolyte).[29] To examine the potential for using thin film RO membranes for water electrolysis applications we compared the performance of two different commercially available RO membranes (BW 30LE and SW 30HR, DuPont) relative to two different commonly used CEMs (Selemion CMV, Asahi Glass; and Nafion 117, Chemours) in terms of membrane resistance and current densities relevant for water electrolyzers. Nafion is commonly referred to as a proton exchange membrane (PEM) when used in electrochemical cells, but it conducts other positively charged cations and therefore it more appropriately referred to here as a CEM.[30] Thin film RO membranes consist of a very thin active layer that selectively restricts large ion transport while permitting water passage under a pressure gradient, and a highly porous structural layer to support the thin film. The side of the membrane with the active layer usually faces the solution with high salinity to maximize desalination performance.[31-33]

Experimental

Membrane resistance measurement

The ionic resistances of the different membranes were measured using a standard four-electrode method at room temperature.[34] All membranes were first immersed in salt solution for 1 day to be equilibrated with the solutions before measurements. The membrane was placed in the middle of cubic shaped cell containing two separate cylindrical chambers. Each chamber filled with 30 mL of a salt solution (NaCl or $NaClO_4$, 0.62 M or 1 M). The membrane area exposed in the aqueous solution was the same as the chamber cross-section (7 cm^2). Platinum coated titanium mesh electrodes (4.4 cm^2) were placed at each end of the cubic cell (10 cm apart). Current was applied across the cell between two electrodes using a potentiostat (VMP3, Bio-Logic). Two Ag/AgCl reference electrodes (BASi RE-5B, West Lafayette, IN) were located directly adjacent to the membrane (1 cm), on each side of the membrane, in order to record the electric potential difference as a function of current density (over a range of 0.06 to 0.6 mA cm^{-2}, normalized by membrane area) using a digital multimeter. The resistance of the membrane, R_M, was determined as follows:

$$R_M = R_{m+sol} - R_{sol}$$

where R_{m+sol} is the resistance of the electrolyte solution measured with the membrane, and R_{sol} is the resistance measured for the electrolyte solution without a membrane. The resistances were determined from the slopes of I-V curves.

Electrochemical measurements

Hydrogen evolution reaction (HER) studies were carried out in a three-electrode system using a potentiostat (VMP3, Bio-Logic) at room temperature. The cells contained a 10% Pt coated carbon paper (10% Pt/C) as the working electrode, a graphite rod counter electrode, and an Ag/AgCl (3M NaCl) reference electrode. The experimentally applied potential vs. Ag/AgCl potentials were converted to SHE using the following equation:

$$E_{SHE} = E_{Ag/AgCl} + 0.197\ V$$

Linear sweep voltammetry (LSV) was carried out at 5 mV s^{-1} between 0 V and –1.4 V (vs. SHE) for the polarization curves. All polarization curves were not iR-compensated. Chronoamperometry (CP) tests were conducted at –1.2V (vs. SHE) for 1 h. The electrolytes were saturated with N_2 purging for 30 min before each test. The volume of each electrolyte was 30 mL in each chamber.

Water electrolysis tests were conducted in a two-electrode system using two identical 10% Pt/C electrodes (1 cm^2) in the same cubic shaped cell with two separate cylindrical chambers. The anode and cathode were separated by the indicated type of membrane. All the current densities for electrolyzer cell performance were normalized by the electrode area (1 cm^2) unless otherwise specified.[35, 36]

Salt crossover measurements

To monitor the cations and anions crossover the different membranes under the same conditions, 1 M of KCl was used as the catholyte and 1 M $NaClO_4$ was used as the anolyte. The two-electrode system was used to apply constant current density (10 mA cm^{-2} or 40 mA cm^{-2}) between anode and cathode for 1 h. The catholyte and anolyte solutions were collected and diluted 50 times to measure salt ion concentrations using ion chromatography (IC, Dionex ICS-1100, Thermo Scientific). Control experiments were conducted under the same conditions but without any applied current. All the measurements were conducted at least two times with different pieces of membrane.

Membrane stability over time

To examine if the transport of ions across the BW membrane was altered over time we conducted chronoamperometry tests at fixed potential of 3.5 or 4.0 V between the anode and cathode for 10 cycles, with 1 hour for each cycle, using a two-electrode setup. Two pieces of BW membrane were used for duplicate tests. To avoid changes in current that could occur due to degradation of the carbon electrodes both electrodes were replaced with new ones for each cycle. KCl (1 M) was used as the catholyte and $NaClO_4$ (1 M) was used as the anolyte. At the end of each cycle, both anolytes and catholytes were collected and diluted 50 times for analysis of the concentration of ions.

Changes in pH over time

During the salt crossover measurements when applying different current density between anode and cathode, the changes in pH of the anolytes and catholytes were monitored simultaneously to observe pH changes during the tests. The final pH was recorded by collecting and mixing the solution. The pH readings will be a little low due to high Na^+ concentration in solution. The pH probes (ET042 pH Electrode, eDAQ, Australia) were calibrated before each measurement with standard buffer solutions.

Gas generation measurements

The generated H_2 and O_2 gases were collected by a drainage method using a lab-made system.[35] The two chambers were sealed with epoxy with electrodes exposed area of 1 cm^2. The two-electrode system was used to apply constant current density of 40 mA cm^{-2} for 1 hour, with 1 M $NaClO_4$ as the anolyte and

1 M NaCl as the catholyte. The gas volume in the cylinder was recorded every 15 min. The Faradaic efficiency was calculated by comparing the amount of collected gas production with theoretical moles of gas using:

$$FE = \frac{n_{H_2}}{n_{CE}}$$

The theoretical moles of H_2 (n_{CE}) that could be recovered based on the measured current with the assumption that all electrons passing through the circuit engage in proton reduction is:

$$n_{CE} = \frac{\int_{i=1}^{n} I_i \Delta t}{2F}$$

where, Δt is the internal time over which current data are collected, and F=96485 C $mole^{-1}$ electron is Faraday's constant. Each mole of H_2 generation requires two moles of electrons.

Results and discussion

Membrane ionic resistances

Electrical current generation in conventional water electrolyzers is enabled by the low resistance of the separator or membrane to ion flow, and thus it is critical that alternative membranes, such as RO membranes, have low resistances comparable to CEMs. Using a standard four-electrode approach to measure membrane resistances,[37] we discovered that certain RO membranes exhibit sufficiently low ionic resistances in highly saline solutions (**Figure S1** and SI). For example, tests using a standard, unmodified brackish water thin film RO membrane (BW), with the active layer facing the cathode (BW/Cat) exhibited a resistance of 21.7 ± 3.5 Ω cm^2 at low current densities (< 1 mA cm^{-2}) in a 1 M NaCl electrolyte and 16.8 ± 4.8 Ω cm^2 in a 1 M $NaClO_4$ electrolyte (**Figure 1a**, **Figure S2**). These resistances were reasonably low but somewhat larger than those measured for the Selemion CEM (Sel) of 4.2 ± 1.2 Ω cm^2 and Nafion 117 (Naf) of 7.2 ± 0.8 Ω cm^2, and a resistance reported (4.89 Ω cm^2, Sel) under the same conditions of 1 M NaCl.[37]

These relatively low RO membrane resistances were not found to be an intrinsic property of all RO membranes. For example, another RO membrane (SW, DuPont Co) had a much larger resistance of 190 ± 75 Ω cm^2 in 1 M NaCl electrolyte and 190 ± 65 Ω cm^2 in 1 M $NaClO_4$ electrolyte with the active layer facing the cathode (SW/Cat). As we discuss below, the low resistances measured here for the BW RO membrane at a low current density (<1 mA cm^{-2}) relative to those desirable for water electrolyzers would not enable the production of large proton gradients on the membrane surface that can be important in maintaining ion balances at higher current densities.

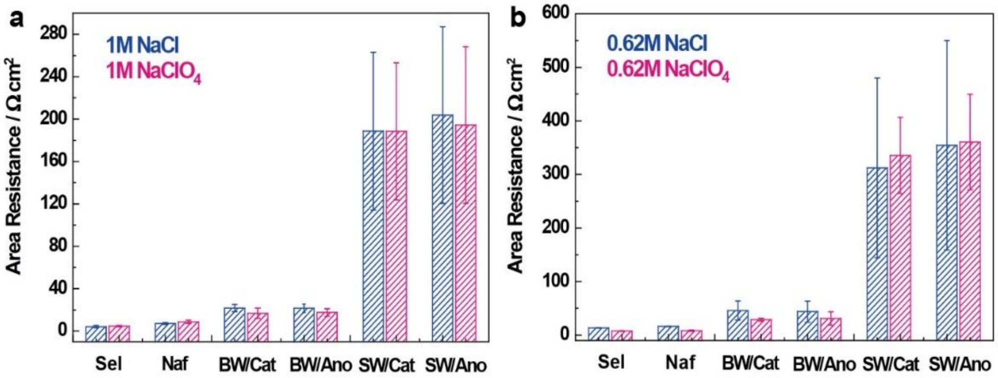

Figure 1. Membrane resistance measured in four-electrode method with different membranes in (a) 1 M NaCl or $NaClO_4$ electrolytes, or (b) 0.62 M NaCl or $NaClO_4$ electrolytes (0.06 to 0.6 mA/cm^2, based on membrane area).

Membrane resistances depended more on the membrane used rather than the orientation of the active layer or the specific electrolyte. Resistances measured using a 1 M $NaClO_4$ electrolyte were similar to those obtained using a 1 M NaCl electrolyte for both RO membranes, independent of membrane orientation (**Figure 1a**). Lowering the electrolyte concentration to that of seawater (0.62 M NaCl) increased the measured resistances for all membranes (**Figure 1b, Figure S2**). The resistances were 13.5 ± 0.3 Ω cm^2 for Sel, 46 ± 18 Ω cm^2 for BW/Cat, and 310 ± 170 Ω cm^2 for SW/Cat in 0.62 M NaCl electrolyte. The lower ionic resistance of BW membranes suggests this membrane is more permeable to ion transport than the SW membrane due to its thinner active layer,[38] which is further examined below. The difference in resistances for the two types of RO membranes suggested that RO membranes could be better designed to enhance ion transport for their use in water electrolyzers; for example, through surface charge modifications or nanoengineering of RO membrane surfaces.[27, 39, 40]

Cell performance with RO membranes

The overall energy requirements for water electrolysis is a function of the applied voltage, which depends on the cell current, membrane resistances, solution resistances and electrode overpotentials. A linear sweep voltammetry (LSV) of a model electrolysis cell with all four membranes showed that Naf produced the highest current densities at a given potential, with the BW/Cat producing the next highest current densities at an applied potential of 3.5 V (**Figure 2a**). At a current density of 10 mA cm^{-2} commonly used to compare overpotentials,[35, 36] similar potentials were required for all cases except for the SW/Cat and SW/Ano conditions. There were larger differences between the BW and SW membranes than those due to the orientation of the active layers (**Figure 2a**). In chronoamperometry (CP) tests at current density of 40 mA cm^{-2}, the required potentials were lowest for the BW/Cat membrane and the Naf compared to the other membranes and test conditions (**Figure 2b**). Differences in measured potentials were primarily due to differences in mass transfer resistances for each ion species, presumably through the membrane, as the same electrode materials (10% Pt/C electrodes) and electrolytes (1 M $NaClO_4$ anolyte and 1 M NaCl catholyte) were used in these tests.

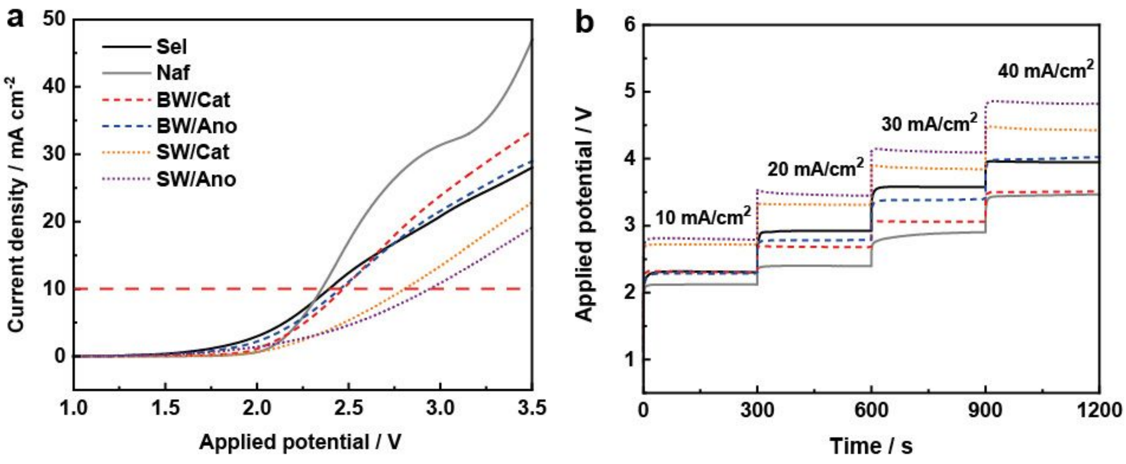

Figure 2. Different membranes in two-electrode system by using two identical 10% Pt/C electrodes as working and counter electrodes using (a) LSV with a scan rate of 5 mV/s, and (b) CP with step current density applied (10, 20, 30 and 40 mA cm^{-2}), with $NaClO_4$ (1 M) anolyte and NaCl (1 M) catholyte.

The choice of using RO membranes or ion exchange membranes will impact the specific ions transported across the membrane, as the RO membrane is selective primarily based on ionic size and mobility, while the CEM will primarily transport cations. Interestingly, these differences did not substantially impact cathode performance based on monitoring the individual electrode reactions. When NaCl was used as the catholyte at a concentration representative of seawater (3.5 wt%, 0.62 M), with the anolyte added at the same mass concentration (3.5 wt%, 0.29 M $NaClO_4$), the cathode potential was –1.0 V vs. SHE at 10 mA cm^{-2} with a Tafel slope of 362 mV/dec for Sel and 340 mV/dec for BW/Cat (**Figure S4**). Using these electrolytes at the same concentration (1 M) decreased the magnitude of applied potential to –0.60 V vs. SHE at 10 mA cm^{-2}, with a decreased Tafel slope of 291 mV/dec for Sel and 236 mV/dec for BW/Cat. The performance of the cathodes used in this study were impacted by solution conditions (**Figure S6**), as shown by a decrease in the Tafel slope to 181 mV/dec for Selemion and 158 mV/dec for BW/Cat membrane by adding a phosphate buffer to the anolyte and catholyte to improve performance. When a Tafel slope is larger than ~120 mV per decade, overall rates are likely limited by mass transfer rather than electrode kinetics.[41] The use of solutions that could be more applicable for a seawater-based electrolyzer (i.e. 0.62 M NaCl catholyte and $NaClO_4$ anolyte) rather than more optimal electrolytes (e.g. higher salt concentrations and buffered solutions) would be expected to reduce mass transport limitations. This comparison of the electrode overpotentials and Tafel slopes does, however, show the similarity of RO and CEM membranes when mass-transport was controlling the performance (i.e. Tafel slopes > 120 mV/dec). An additional chronoamperometry experiment was conducted using 0.62 M NaCl in both chambers for 1 h at –1.2 V vs. SHE applied potential (for cathode), producing a current density of 60-90 mA cm^{-2} **(Figure S5**). In these tests there was clear evidence of damage to the Selemion membrane due to chlorine evolution from Cl^- oxidation in the anolyte, consistent with other studies.[20] In contrast, there was no observable membrane damage under the same conditions using the 0.62 M $NaClO_4$ anolyte. This experiment provided direct evidence that evolution of reactive, oxidized chlorine species can be avoided by choosing a contained and unreactive anolyte.

Figure 3. LSV measurement for different membranes in three-electrode system with 10% Pt/C working electrode, graphite rod counter electrode, and Ag/AgCl reference electrode with the indicated anolyte and catholyte solution: (a) 3.5% NaCl (0.29 M NaCl) catholyte and 3.5% $NaClO_4$ (0.62 M) anolyte, (b) 1 M NaCl catholyte and 1 M $NaClO_4$ anolyte, and (c) 1 M NaCl catholyte and 1 M $NaClO_4$ anolyte in 1 M phosphate buffer solution (PBS).

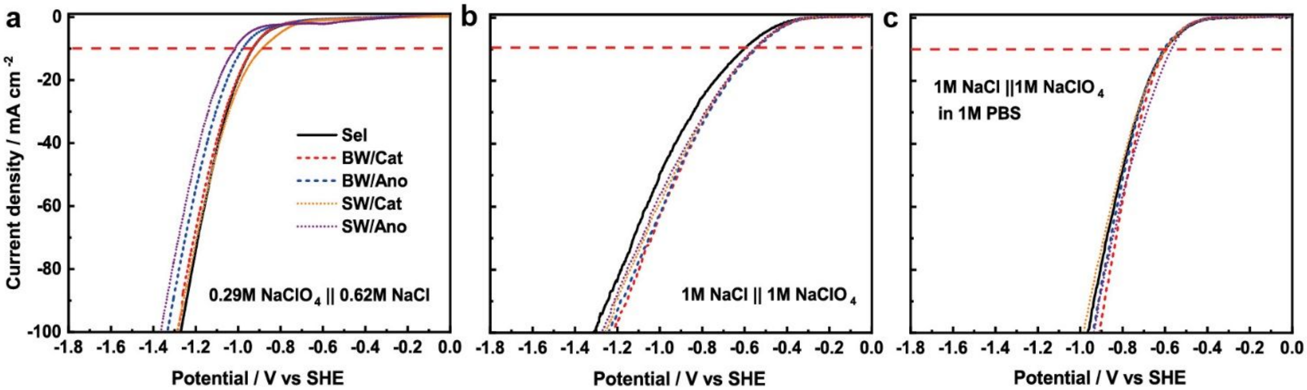

Transport of electrolyte salts across membranes

CEMs are designed to facilitate cation transport, but RO membranes selectively transport smaller ions, and therefore transport of larger cations such as Na^+ could be reduced relative to protons for RO membranes under comparable solution conditions and current densities. RO membranes are not perfectly selective for ion transport, however, and there will be some crossover of larger ions due to membrane pore size variability and defects due to diffusion as a result of the large concentration gradient and the electric field. To examine the extent of cation crossover in the presence and absence of an electric field, we used sodium perchlorate in the anolyte and potassium chloride in the catholyte (1 M $NaClO_4$ anolyte and 1 M KCl catholyte) at set current densities of 10 and 40 A m^{-2}, and compared the concentration of each ion after one hour to the control (no current **Figure S8**). Na^+ ions were transported to a greater extent than other ions due to the concentration gradient (no current) for CEMs compared to RO membranes, and total Na^+ ion transport increased in proportion to the current (**Figure 4**). With only the concentration difference (no current), the final Na^+ concentrations in catholyte were higher using CEMs than RO membranes, with 26.3 ± 2.8 mM for Sel and 13.4 ± 1.3 mM for Naf, with Na^+ concentrations < 1.2 mM for the RO membranes (1.02 ± 0.17 mM for BW/Cat and 0.64 ± 0.04 mM for SW/Cat; **Figure S8**). This same trend of increased Na^+ transport with CEMs compared to RO membranes was observed with electric field applied. At 40 A m^{-2}, the transport of Na^+ in the direction of the electric field (i.e. towards the cathode) led to 62 ± 8 mM of Na^+ (Sel) and 48±2 mM (Naf), compared to a lower range of 17.5 ± 1.6 mM (SW/Cat) to 19.3 ± 2.1 mM (BW/Cat) for the RO membranes (**Figure 4**). These salt concentrations were reduced with a lower current of 10 A m^{-2} (42.4 ± 4.8 mM, Sel, 18.5 ± 4.9 mM, Naf, compared to 6.09 ± 0.13 mM, BW/Cat, 5.59 ± 0.35 mM for SW/Cat), indicating enhanced Na^+ ion transport due to the electric field. Because ion transport in solution is needed to balance the same applied current, these results indicated that the charge balance was maintained by ions other than Na^+ to a greater extent in the RO membranes than in the CEMs.

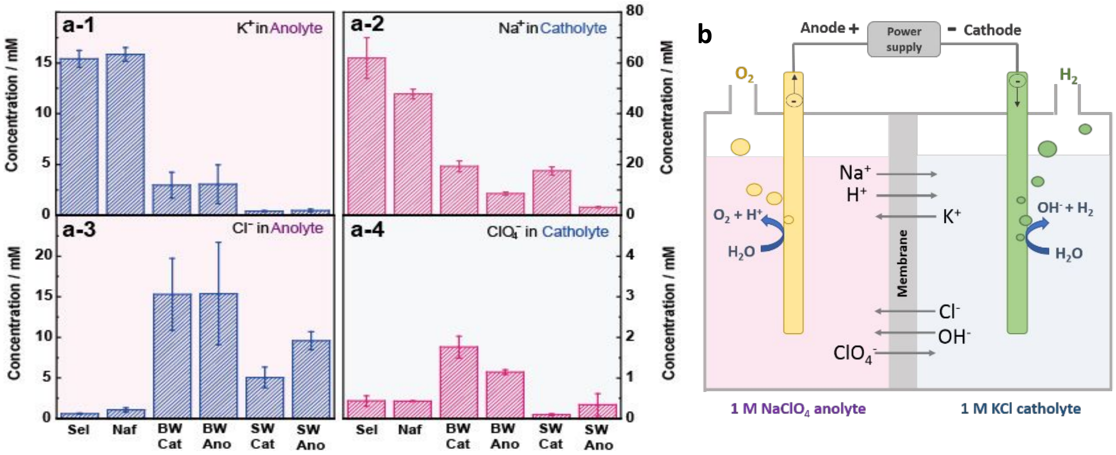

Figure 4. (a) Concentration of cations and anions in cell using different membranes after applying a constant current of 40 mA cm^{-2} between anode and cathode for 1 h: K^+ concentration in anolyte (a-1) and Na^+ in catholyte (a-2), Cl^- in anolyte (a-3) and ClO_4^- in catholyte (a-4). K^+ in catholyte, Na^+ in anolyte, Cl^- in catholyte and ClO_4^- in anolyte were presented in Figure S7. Schematic figure (b) showing ions moving under constant current, with original solution of KCl (1 M) for catholyte and $NaClO_4$ (1 M) for anolyte. KCl was used instead of NaCl (as synthetic seawater) for catholyte in order to indicate the cations transport under different conditions.

The electric field only had a small effect on K^+ ion transport towards against the electric field (towards the anode) with all membranes, indicating most of K^+ transport was likely due to diffusion not migration. There was still greater K^+ ion transport with the CEMs (15.4 ± 0.8 and 8.0 ± 1.6 mM, Sel) than the RO membranes (2.9 ± 1.2 and 0.59 ± 0.13 mM, BW/Cat) (**Figures 4, S8, and S9**), both with and without an electric field. Diffusion of K^+ or Na^+ into the opposing electrolyte therefore was due to the large concentration gradients between the two chambers, with greater transport against the electric field due to the higher permeability of positively charged cations through the CEMs.

Anion transport was enhanced in the direction of the electric field (towards the anolyte) using RO membranes compared to CEMs which better restrict anion transport. After 1 hour there was 5.1 ± 1.2 mM (SW/Cat) and 15.3 ± 4.4 mM (BW/Cat) of Cl^- in the anolyte at 40 mA cm^{-2}, compared to <0.6 mM for the CEMs in all cases (with or without current). Chloride transport was enhanced by the electric field as there was <1mM accumulation of Cl^- in control experiments with no current (0.10 ± 0.01 mM, SW/Cat; 0.98 ± 0.09 mM, BW/Cat). For ClO_4^-, ion transport against the electric field resulted in a range of 1.76 ± 0.26 mM (BW/Cat) to 0.09 ± 0.02 mM (SW/Cat) in the catholyte for the RO membranes with 40 mA cm^{-2}. However, in other tests at 10 mA cm^{-2} **(Figure S9)**, there was little overall enhanced perchlorate ion transport out of the anolyte indicating its transport through the membrane was mainly by diffusion.

The fraction of charge that was carried through the membrane to maintain charge balance when a current is applied was calculated by performing an ionic charge balance using the data in **Figure 4**. Proton production in the anode chamber reduces the anolyte pH, and hydroxide production in the catholyte chamber increases the catholyte pH, as observed for both CEM and RO membranes (**Figure S10**). The maximum proton concentration in the anolyte was calculated assuming that 100% of the current led to proton production with a $1H^+:1e^-$ ratio, and that no protons were transported through the membrane (Max, **Figure 5a**). Based on the set current (40 mA cm^{-2}) the maximum possible proton concentration was 49.7 mM in anolyte. The calculated value was generated by performing a charge balance calculation (Ion balance, **Figure 5a,** SI), and the measured concentrations were obtained using a pH electrode of the final electrolyte (Measured, **Figure 5a**). The calculated proton concentrations remaining in the anolyte were higher than those measured, indicating additional ion transport occurred between the electrolyte chambers either due to ion swapping reactions or membrane imperfections. The measured remaining proton concentrations in the anolyte for all membranes, converted from the measured pH values of final anolytes (**Figure S11**), were much lower than this maximum, with 27.9 mM for Sel, 22.2 mM for Naf, 13.7 for BW/Cat and 20.0 mM for SW/Cat, supporting the passage of protons through both CEMs and RO membranes due to the imposed electric field (**Figure 5a**).

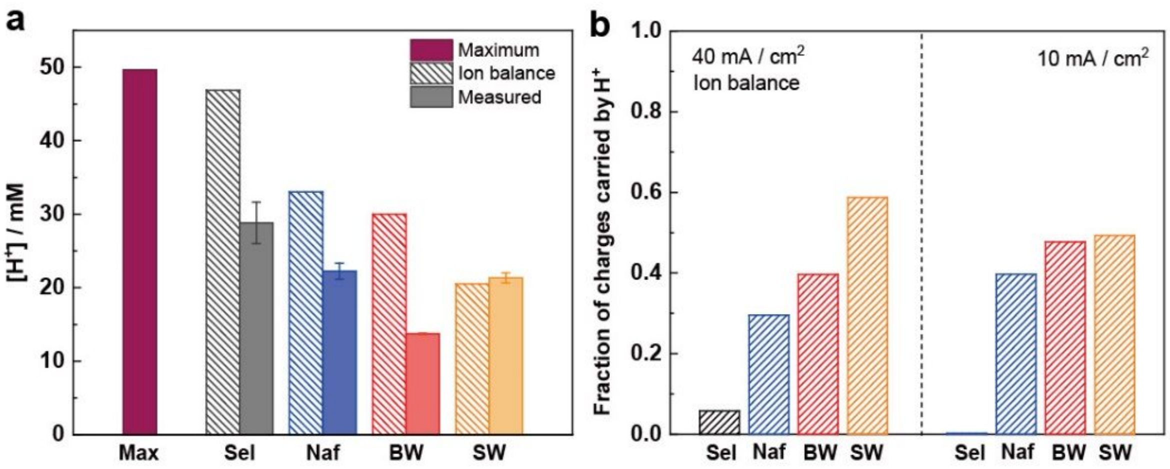

Figure 5. (a) Proton concentrations in the anolyte for different conditions, assuming a 100% Faradaic efficiency (40 mA cm^{-2} for 1 h): maximum proton concentration for no proton transport through membrane (Max); proton concentrations remaining based on measured ion transport of other salt species (Ion balance) and proton concentrations converted from measured pH values at the end of the experiment (Measured). (b) The fraction of charge carried by protons transported through different membranes to sustain the current density of 40 mA cm^{-2} or 10 mA cm^{-2} for 1 h (1 M $NaClO_4$ anolyte and 1 M KCl catholyte).

Based on these experiments and additional tests conducted under a lower applied current density (10 mA cm^{-2}), we concluded that the selectivity of proton transport is larger for the RO membranes than for the CEMs (**Figure 5b and Figure S12**). For example, 0.08 mmol of protons were transferred through the

Sel membrane, or 5% of the total charges (1.49 mmol) needed to balance charge at 40 mA cm^{-2}. For the RO membranes, 0.6 mmol or 40% of the total charge was proton for the BW/Cat configuration, and 0.88 mmol or 59% for SW/Cat configuration at 40 mA cm^{-2} (details of the calculation are provided in the SI).

An additional concern is membrane stability over time in the electrolytes. The stability of the BW membrane relative to maintaining a constant current and changes in passage of ions over time was examined by applying a constant potential of 3.5 V for 5 cycles, followed by 5 more cycles with 4.0 V across the anode and the cathode (10 cycles total, each 1 h long). Examination of the changes in total ions transferred showed that ions transported against the electric field (ClO_4^- and K^+) did not increase in concentration over time based on the lack of significance of the slopes (all with $p>0.05$) for the final concentrations at the end of each cycle over time (**Figure 6**), consistent with the results in **Figure 4** (additional data in **Figure S13**). The diffusion of perchlorate and potassium ions was similar in amount over all the data suggesting that the active layer was not impaired during the tests. For the two ions transported in the direction of the electric field (Na^+ and Cl^-) the mass of ions transported there was a slight increase in Cl^- ion transport at 3.5 V ($p=0.005$) but not at 4.0 V d ($p=0.101$). For Na^+ ion transport at both applied voltages there was a small but significant ($p=0.027$, 3.5 V; $p<0.001$, 4.0 V) increase in ion transport over time. The reason for this increase was not clear, and this phenomenon requires further investigation. A longer period of time was not examined here as the carbon electrodes used here oxidize over time and thus the system can have changes in performance unrelated to the membrane stability but due to chemical reactions on the carbon electrodes that might impact membrane stability and performance.[42]

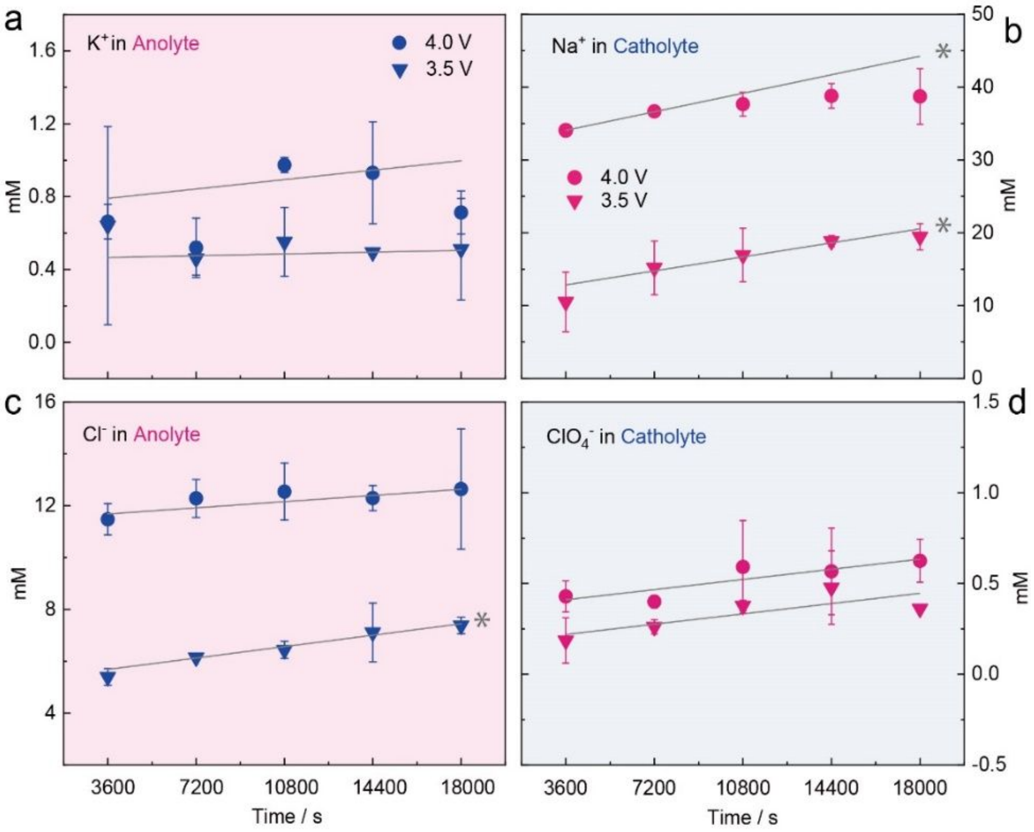

Figure 6. The concentration of cations and anions using BW membranes after applying constant potentials of 3.5 V and then 4.0 V (total of 10 cycles, with 1 hour for each cycle): (a) K^+ concentration in anolyte, (b) Na^+ in catholyte, (c) Cl^- in anolyte, and (d) ClO_4^- in the catholyte. Two pieces of BW membrane were used for duplicate tests. The * shows that the slope of the linear regression was significant at the $p<0.05$ level. Details of the statistical analysis are summarized in Table S1.

Faradaic product efficiency of the seawater electrolysis

A water displacement gas collection system was used to collect the gases produced by the cathode and anode to evaluate gas recoveries for practical applications and Faradaic efficiencies (**Figure 7**). Gas collection tests were conducted using a 1 M NaCl catholyte and 1 M $NaClO_4$ anolyte. At a set current density of 40 mA cm^{-2} for 1 h, H_2 and O_2 were produced at the expected molar ratio (2.13±0.09:1) (**Figure 7a**). A total of 16.0 ± 0.2 mL H_2 was obtained within 1 h, showing a Faradaic efficiency of >95 % in all tests with the different membranes. The smaller Faradaic efficiency for O_2 evolution could have been due to carbon corrosion of the anode which was not optimized for these membrane-based tests (**Figure 7b**).[42]

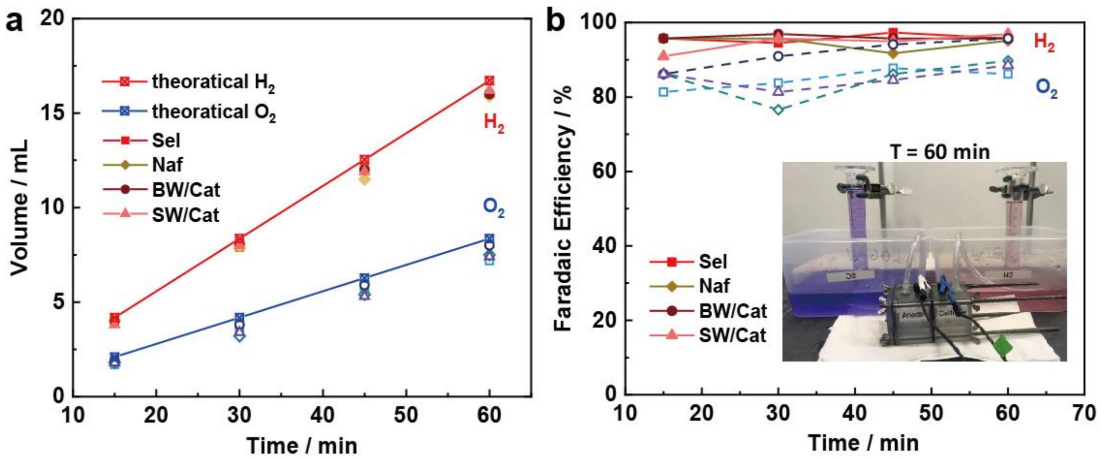

Figure 7. **(**a) Volume of generated H_2 and O_2 at a constant current of 40 mA cm^{-2} for 1 h with 1 M $NaClO_4$ anolyte and 1 M NaCl catholyte. (b) Faradaic efficiency of H_2 and O_2 evolution. The inset picture is the lab-made system with cylinders capturing the gases from the anode and cathode filled with colored water to make the water lines more visible (shown for an experiment with the BW/Cat membrane after 1 h of collection).

Engineering RO membranes to function more efficiently in salty water electrolyzers.

There is a well-known tradeoff in RO membranes relative to selectivity versus permeability for water flux,[27, 28, 39, 43] but this relationship has not been sufficiently examined in the presence of an electric field across the membrane and in the absence of bulk water flow. CEMs achieve selective charge transport of cations over anions, but RO membranes have the advantage of size exclusion to aid transport of protons compared to larger cations. Thus, it was shown here that more Na^+ and K^+ cations were transferred by CEMs in the presence or absence of current compared to RO membranes (**Figure 4**). Furthermore, an ion balance demonstrated greater proportion of protons transported through the RO membranes to balance charge than the other ions (**Figure 5**). Ion transport and ion selectivity in the active layer of an RO membrane, in the absence of pressure-driven water flow, is not understood from the perspective of charge balance when proton transport is favored over larger ion transport (e.g. chloride). Ion transport through separators that are either nonselective or selective on the sizes of large molecules (for example in nanofiltration or ultrafiltration membranes) is fundamentally different from that through RO membranes which are size selective on the scale of molecular radius. Due to the need for charge balance on both sides of the RO membrane and the high proton generation rate at the anode, the proton gradient at the surface of an RO membrane during water electrolysis is unlike previously studied situations without current generation for situations comparable to nanofiltration membranes where ion transport is due primarily to pressure forces.[44]

Greater selective transport of protons in RO membranes could be achieved through two approaches: reducing defects and adjusting the charge of the membrane surface. The surface charge of RO membranes can be varied. The BW membrane used here has been reported to have a more positive surface charge of the active layer at lower pHs and a more negative surface charge of the active layer at higher pHs than the SW membrane.[22, 45] The negative surface charge is believed to be favorable for protons transport,[22] consistent with our results (**Figure 2**). When the active layer of the RO membrane faced the catholyte that had a higher pH (BW/Cat and SW/Cat), the overpotential was lower than that obtained with the active layer facing the anolyte which had a lower pH (BW/Ano and SW/Ano). RO membrane coatings, such as polyethylene glycol, polyvinyl acetate, polydopamine, and other strategies have been used to accomplish surface charge engineering of RO and FO membranes.[46] The BW membrane is also more permeable due to less polyamide cross-linking than the SW membrane, which could account for greater diffusional transport of all ions using the BW membrane. [18, 19] Therefore, there is much that can be done to better engineering RO and FO membranes to function more effectively for desirable small ion transport in water electrolyzer systems.

Another challenge for using RO membranes with seawater is controlling loss of anolyte salts into the catholyte. Sodium perchlorate salts were used here as they are known to be electrochemically stable as they do not lead to more oxidized forms of chlorine. However, other salts could be investigated for the purpose of providing an electrochemically stable environment such as sulfate or other compounds. An additional concern would be whether pH levels became too acidic (<2) in the anolyte or too alkaline (>11) in the catholyte as these could lead to damage of the membrane.[21] A low pH can lead to appreciable concentrations of perchloric acid which could potentially damage the polyamide layer, but there is little known about the impact of perchlorate on RO membranes. Others have used thin film polyamide membranes in 3 M H_2SO_4, but they did not report on membrane stability.[29] Compared to other predominant chlorine species (e.g. Cl_2, HOCl and OCl^-) perchlorate is the least effective oxidizer.[47] There will always be some loss of ions from the anolyte into the catholyte as RO membranes do not completely reject salts. However, even if it is not possible to completely eliminate perchlorate transfer into the catholyte, the removal of perchlorate through biological treatment is a relatively simple process.[48-51] Amending the solution with a substrate such as acetate or even dissolved hydrogen can enable the rapid reduction of perchlorate to chloride in several different types of systems including packed beds, fluidized beds, and hollow fiber membrane bioreactors.[49, 52-56]

The main research approach for directly using seawater has been to focus on using electrode materials that favor the oxygen evolution reaction (OER) over chloride oxidation.[12-14] For example, a porous manganese-based electrode was first proposed to selectively enhance the OER in acidic solutions.[57] It has also been shown that deposition of MnO_x onto IrO_x enhances OER selectivity by a blocking mechanism, in which the MnO_2 prevents Cl^- from reaching the catalytically active IrOx.[58] NiFe-based (oxy) hydroxides are currently considered to be one of the most efficient OER catalysts among different non-noble metal catalysts in alkaline electrolytes.[59] A multilayer anode of a nickel-iron hydroxide (NiFe) electrocatalyst layer coated on a nickel sulfide (NiSx) layer formed on porous Ni foam (NiFe/NiSx-Ni) can afford superior catalytic activity and corrosion resistance in solar-driven alkaline seawater electrolysis.[60] A sandwich-like nanostructured HER catalyst by decorating both sides of nickel phosphide microsheet arrays with nickel cobalt nitride nanoparticles was recently produced to possess impressive stability benefiting from the good chlorine-corrosion resistance in neutral pH seawater.[61] These advances in electrode materials will be especially useful when used in concert with an RO membrane as chloride ion transport cannot be completely eliminated. The leakage of some chloride ions, combined with electrodes that selectively enhance the OER over chloride oxidation, will result in a more robust and effective process.

The use of RO or FO membranes in water electrolyzers can have additional benefits other than very low costs compared to CEMs. For example, they could be used to directly provide water into the anolyte chamber to replenish that lost during water electrolysis and like CEMs that are effective at preventing gas transfer between the chambers. A current density of 100 mA cm^{-2} requires a water flux of 0.34 L m^{-2} h^{-1} (LMH). By altering the anolyte concentration to act as a draw solution, or through adjusting pressure in the two chambers, it should be possible to add additional water source into the anolyte chamber. This procedure to add water might be best conducted in the absence of current generation to avoid carryover of dissolved H_2 into the anode chamber. Just like a CEM, the RO membrane is not just a separator of ions, it can also avoid gas phase transfer between the chambers,[62] which is used in CEM water electrolyzers to enable higher pressure hydrogen gas production, but not in alkaline water electrolyzers that usually use a separator which is more permeable to gas transport.

Conclusions

This study presented a first proof-of-concept design by using RO membrane based electrolyzer for direct seawater H_2 generation with inert anolyte. By comparing two types of RO membranes (BW and SW) and two types of ion exchange membranes (CEM and Nafion 117), it was found that BW membrane has acceptable performance over the membrane resistance and electrolysis over potential. Overall, there remain challenges for using ion excluding thin film composite membranes such as RO membranes compared to ion exchange membranes that facilitate transport of all like-charged ions. However, the overall cost of the RO membranes compared to ion exchange membranes provides incentive to explore their use in water electrolyzer systems. While the main focus of the studies here is to enable the direct use of seawater in these systems, the comparison between RO membrane and IEM on transport of protons and salt ions in electric field showed that RO membranes possessed promising selectivity of protons over cation salts when using high concentrated electrolytes and the polyamide based thin-film composite membrane as presented here should provide opportunities for their use in conventional water electrolyzer systems based on the use of alkaline solutions.

Conflicts of Interest

There are no conflicts to declare.

Acknowledgments

This research was funded by the Stan and Flora Kappe endowment, Penn State University, the National Science Foundation grant CBET-2027552, and by USAID and NAS through Subaward 2000010557. Any opinions, findings, conclusions, or recommendations expressed in this article are those of the authors alone, and do not necessarily reflect the views of USAID or NAS.

References

1. Essential Chemical Industry, http://www.essentialchemicalindustry.org/chemicals/hydrogen.html, (accessed May 7, 2020).
2. B. E. Logan, *Environ. Sci. Technol. Lett.*, 2019, **6**, 257-258.
3. D. V. Esposito, *Joule*, 2017, **1**, 651-658.
4. A. T. Mayyas, M. F. Ruth, B. S. Pivovar, G. Bender and K. B. Wipke, *Manufacturing cost analysis for proton exchange membrane water electrolyzers*, Report NREL/TP-6A20-72740 United States 10.2172/1557965 NREL English, ; National Renewable Energy Lab. (NREL), Golden, CO (United States), 2019.
5. S. Dresp, F. Dionigi, S. Loos, J. Ferreira de Araujo, C. Spöri, M. Gliech, H. Dau and P. Strasser, *Adv. Energy Mat.*, 2018, **8**, 1800338.
6. S. Dresp, F. Dionigi, M. Klingenhof and P. Strasser, *ACS Energy Lett.*, 2019, **4**, 933-942.
7. W. Tong, M. Forster, F. Dionigi, S. Dresp, R. Sadeghi Erami, P. Strasser, A. J. Cowan and P. Farràs, *Nature Energy*, 2020, DOI: 10.1038/s41560-020-0550-8.
8. Y. Yang, J. Shin, J. T. Jasper and M. R. Hoffmann, *Environ. Sci. Technol.*, 2016, **50**, 8780-8787.
9. M. Stolov and V. Freger, *Environ. Sci. Technol.*, 2019, **53**, 2618-2625.
10. K. E. Ayers, E. B. Anderson, C. Capuano, B. Carter, L. Dalton, G. Hanlon, J. Manco and M. Niedzwiecki, *ECS Transactions*, 2019, **33**, 3-15.
11. M. Bernt, A. Hartig-Weiß, M. F. Tovini, H. A. El-Sayed, C. Schramm, J. Schröter, C. Gebauer and H. A. Gasteiger, *Chemie Ingenieur Technik*, 2020, **92**, 31-39.
12. F. Dionigi, T. Reier, Z. Pawolek, M. Gliech and P. Strasser, *ChemSusChem*, 2016, **9**, 962-972.
13. S.-H. Hsu, J. Miao, L. Zhang, J. Gao, H. Wang, H. Tao, S.-F. Hung, A. Vasileff, S. Z. Qiao and B. Liu, *Advanced Materials*, 2018, **30**, 1707261.
14. R. K. B. Karlsson and A. Cornell, *Chem. Rev.*, 2016, **116**, 2982-3028.
15. S. Dresp, T. Ngo Thanh, M. Klingenhof, S. Brückner, P. Hauke and P. Strasser, *Energy Env. Sci.*, 2020, **13**, 1725-1729.
16. S. K. Jeong, J. S. Lee, S. H. Woo, J. A. Seo and B. R. Min, *Energies*, 2015, **8**, 7084-7099.

17. J. Fan, S. Willdorf-Cohen, E. M. Schibli, Z. Paula, W. Li, T. J. G. Skalski, A. T. Sergeenko, A. Hohenadel, B. J. Frisken, E. Magliocca, W. E. Mustain, C. E. Diesendruck, D. R. Dekel and S. Holdcroft, *Nature Commun.*, 2019, **10**, 2306.
18. S.-J. Kim, S. Kook, B. E. O'Rourke, J. Lee, M. Hwang, Y. Kobayashi, R. Suzuki and I. S. Kim, *J. Mem. Sci.*, 2017, **527**, 143-151.
19. S.-J. Kim, D. Han, H.-W. Yu, B. E. O'Rourke, Y. Kobayashi, R. Suzuki, M. Hwang and I. S. Kim, *Desal.*, 2018, **432**, 104-114.
20. M. Son, T. Kim, W. Yang, C. A. Gorski and B. E. Logan, *Environ. Sci. Technol.*, 2019, **53**, 8352-8361.
21. Dupont, *FilmTec™ reverse osmosis membranes technical manual*, 2020.
22. K. Kezia, J. Lee, W. Ogieglo, A. Hill, N. E. Benes and S. E. Kentish, *J. Mem. Sci.*, 2014, **459**, 197-206.
23. P. Nativ, N. Fridman-Bishop and Y. Gendel, *J. Mem. Sci.*, 2019, **584**, 46-55.
24. V. Freger and S. Bason, *J. Mem. Sci.*, 2007, **302**, 1-9.
25. S. Bason, Y. Oren and V. Freger, *J. Mem. Sci.*, 2007, **302**, 10-19.
26. S. Bason, Y. Oren and V. Freger, *J. Mem. Sci.*, 2011, **367**, 119-126.
27. J. R. Werber, A. Deshmukh and M. Elimelech, *Environ. Sci. Technol. Lett.*, 2016, **3**, 112-120.
28. G. M. Geise, M. A. Hickner and B. E. Logan, *ACS Appl. Mat. Interfac.*, 2013, **5**, 10294-10301.
29. Q. Dai, Z. Liu, L. Huang, C. Wang, Y. Zhao, Q. Fu, A. Zheng, H. Zhang and X. Li, *Nature Commun.*, 2020, **11**, 13.
30. K. Hongsirikarn, J. G. Goodwin, S. Greenway and S. Creager, *J. Power Sources*, 2010, **195**, 7213-7220.
31. G. T. Gray, J. R. McCutcheon and M. Elimelech, *Desal.*, 2006, **197**, 1-8.
32. M. Elimelech and W. A. Phillip, *Science*, 2011, **333**, 712-717.
33. T. Y. Cath, M. Elimelech, J. R. McCutcheon, R. L. McGinnis, A. Achilli, D. Anastasio, A. R. Brady, A. E. Childress, I. V. Farr, N. T. Hancock, J. Lampi, L. D. Nghiem, M. Xie and N. Y. Yip, *Desal.*, 2013, **312**, 31-38.
34. G. M. Geise, A. J. Curtis, M. C. Hatzell, M. A. Hickner and B. E. Logan, *Environmental Science & Technology Letters*, 2014, **1**, 36-39.
35. C. Bai, S. Wei, D. Deng, X. Lin, M. Zheng and Q. Dong, *Journal of Materials Chemistry A*, 2017, **5**, 9533-9536.
36. J. Lai, S. Li, F. Wu, M. Saqib, R. Luque and G. Xu, *Energy Env. Sci.*, 2016, **9**, 1210-1214.
37. G. M. Geise, A. J. Curtis, M. C. Hatzell, M. A. Hickner and B. E. Logan, *Environ. Sci. Technol. Lett.*, 2014, **1**, 36-39.
38. N. Fridman-Bishop and V. Freger, *J. Mem. Sci.*, 2017, **540**, 120-128.
39. A. P. Straub, C. O. Osuji, T. Y. Cath and M. Elimelech, *Environ. Sci. Technol.*, 2015, **49**, 12551-12559.
40. X.-H. Ma, Z.-K. Yao, Z. Yang, H. Guo, Z.-L. Xu, C. Y. Tang and M. Elimelech, *Environ. Sci. Technol. Lett.*, 2018, **5**, 123-130.
41. M. Chatenet, J. Benziger, M. Inaba, S. Kjelstrup, T. Zawodzinski and R. Raccichini, *J. Power Sources*, 2020, **451**, 227635.
42. L. M. Roen, C. H. Paik and T. D. Jarvi, *Electrochemical and Solid-State Letters*, 2004, **7**, A19.
43. G. M. Geise, D. R. Paul and B. D. Freeman, *Progress in Polymer Science*, 2014, **39**, 1-42.
44. J. Wang, D. S. Dlamini, A. K. Mishra, M. T. M. Pendergast, M. C. Y. Wong, B. B. Mamba, V. Freger, A. R. D. Verliefde and E. M. V. Hoek, *J. Mem. Sci.*, 2014, **454**, 516-537.
45. E. Idil Mouhoumed, A. Szymczyk, A. Schäfer, L. Paugam and Y. H. La, *J. Mem. Sci.*, 2014, **461**, 130-138.
46. G. Hurwitz, G. R. Guillen and E. M. V. Hoek, *J. Mem. Sci.*, 2010, **349**, 349-357.
47. F. A. Cotton and G. Wilkinson, *Advanced Inorganic Chemistry (5th ed.)*, Wiley-Interscience, 1988.

48. B. E. Logan, J. Wu and R. F. Unz, *Water Res.*, 2001, **35**, 3034-3038.
49. S. G. Lehman, M. Badruzzaman, S. Adham, D. J. Roberts and D. A. Clifford, *Water Res.*, 2008, **42**, 969-976.
50. S. Sevda, T. R. Sreekishnan, N. Pous, S. Puig and D. Pant, *Bioresour. Technol.*, 2018, **255**, 331-339.
51. P. B. Hatzinger, *Environ. Sci. Technol.*, 2005, **39**, 239A-247A.
52. J. C. Brown, R. D. Anderson, J. H. Min, L. Boulos, D. Prasifka and G. J. G. Juby, *Journal - AWWA*, 2005, **97**, 70-81.
53. B. E. Logan and D. LaPoint, *Water Res.*, 2002, **36**, 3647-3653.
54. R. Nerenberg, B. E. Rittmann and I. Najm, *Journal American Water Works Association*, 2002, **94**, 103-114.
55. B. Min, P. J. Evans, A. Chu and B. E. Logan, *Water Res.*, 2004, **38**, 47-60.
56. H. Zhang, M. A. Bruns and B. E. Logan, *Environ. Microbiol.*, 2002, **4**, 570-576.
57. J. E. Bennett, *Int. J. Hydrogen Energy*, 1980, **5**, 401-408.
58. J. G. Vos, T. A. Wezendonk, A. W. Jeremiasse and M. T. M. Koper, *J. Am. Chem. Soc.*, 2018, **140**, 10270-10281.
59. L. Yu, L. Wu, B. McElhenny, S. Song, D. Luo, F. Zhang, Y. Yu, S. Chen and Z. Ren, *Energy Env. Sci.*, 2020, DOI: 10.1039/D0EE00921K.
60. Y. Kuang, M. J. Kenney, Y. Meng, W.-H. Hung, Y. Liu, J. E. Huang, R. Prasanna, P. Li, Y. Li, L. Wang, M.-C. Lin, M. D. McGehee, X. Sun and H. Dai, *Proc. Nat. Academy Sci.*, 2019, **116**, 6624-6629.
61. L. Yu, L. Wu, S. Song, B. McElhenny, F. Zhang, S. Chen and Z. Ren, *ACS Energy Lett.*, 2020, **5**, 2681-2689.
62. J. S. Louie, I. Pinnau and M. Reinhard, *J. Mem. Sci.*, 2008, **325**, 793-800.

Broader context

Hydrogen gas generation is essential for fertilizer production and other uses, but it currently is a major contributor to greenhouse gas emissions from fossil fuels. Hydrogen gas can be produced through water electrolysis and renewable solar or wind energy, but capital costs for water electrolyzers need to be reduced. Offshore and coastal sites for hydrogen production are good locations for obtaining inexpensive wind and solar energy and abundant seawater, but chloride ions in seawater generate toxic chlorine gas that damages water electrolyzer membranes. It is shown here that reverse osmosis membranes used for seawater desalination are highly permeable to proton transport, and thus provide performance that is similar to ion exchange membranes that are 10 to 100 times more expensive. RO membranes pass protons through small pores that are efficient at exclusion of larger ions. Therefore, they can be used to contain salts in anolyte that do not generate chlorine gas, while seawater can be used in the catholyte for hydrogen gas production. These results show that that by using appropriate RO membranes and anolyte, the costs of water electrolysis membranes can be reduced while facilitating the use of contained electrolytes that avoid unwanted chemical reactions.